Electron Vortices in Photoionization by Circularly Polarized Attosecond Pulses

J. M. Ngoko Djiokap,[1] S. X. Hu,[2] L. B. Madsen,[3] N. L. Manakov,[4] A. V. Meremianin,[4] and Anthony F. Starace[1]
[1]Department of Physics and Astronomy, University of Nebraska, Lincoln, Nebraska 68588-0299, USA
[2]Laboratory for Laser Energetics, University of Rochester, Rochester, New York 14623-1299, USA
[3]Department of Physics and Astronomy, Aarhus University, DK-8000 Aarhus C, Denmark
[4]Department of Physics, Voronezh State University, Voronezh 394006, Russia
(Received 4 May 2015; revised manuscript received 1 July 2015; published 10 September 2015)

Single ionization of He by two oppositely circularly polarized, time-delayed attosecond pulses is shown to produce photoelectron momentum distributions in the polarization plane having helical vortex structures sensitive to the time delay between the pulses, their relative phase, and their handedness. Results are obtained by both *ab initio* numerical solution of the two-electron time-dependent Schrödinger equation and by a lowest-order perturbation theory analysis. The energy, bandwidth, and temporal duration of attosecond pulses are ideal for observing these vortex patterns.

DOI: 10.1103/PhysRevLett.115.113004 PACS numbers: 32.80.Fb, 02.70.Dh, 02.70.Hm, 03.75.-b

Ramsey interference [1] of laser-produced electron wave packets has been investigated in both Rydberg states [2,3] and in the continuum [4] for the case of linearly polarized lasers. In this Letter we investigate an unusual kind of Ramsey interference between photoelectron wave packets produced in ionization of the helium atom by a pair of time-delayed, oppositely circularly polarized, attosecond laser pulses. In the polarization plane, the photoelectron momentum distributions exhibit helical vortex patterns, corresponding to Fermat spirals, whose handedness depends on whether the pair of attosecond pulses are right-left or left-right circularly polarized. Observation of the vortex patterns requires the large bandwidth of few-cycle attosecond pulses. Moreover, the vortex patterns in the photoelectron momentum distributions that we predict have a counterpart in optics [5], in which similar vortex patterns have been produced by interference of particular kinds of laser beams. Our predicted photoelectron momentum distributions thus provide an example of wave-particle duality, and our predicted angular distributions demonstrate an unusual kind of control over photoelectrons on an attosecond time scale.

Consider the interaction of the helium atom in its $^1S^e$ ground state with the electric field $\boldsymbol{F}(t)$ of a pair of attosecond pulses having the same carrier frequency ω and smooth pulse envelope $F_0(t)$, but differing in their polarizations $\mathbf{e}_{1,2}$ and carrier envelope phases (CEPs) $\phi_{1,2}$, with the second pulse delayed in time by τ, i.e.,

$$\boldsymbol{F}(t) = \boldsymbol{F}_1(t) + \boldsymbol{F}_2(t-\tau) \equiv F_0(t)\mathrm{Re}[\mathbf{e}_1 e^{-i(\omega t+\phi_1)}] + F_0(t-\tau)\mathrm{Re}[\mathbf{e}_2 e^{-i(\omega(t-\tau)+\phi_2)}]. \quad (1)$$

For the jth pulse ($j = 1, 2$), the polarization vector is $\mathbf{e}_j \equiv (\hat{\boldsymbol{\epsilon}} + i\eta_j\hat{\boldsymbol{\xi}})/\sqrt{1+\eta_j^2}$, where η_j is the ellipticity ($-1 \le \eta_j \le +1$), $\hat{\boldsymbol{\epsilon}}$ and $\hat{\boldsymbol{\xi}} \equiv \hat{\mathbf{k}} \times \hat{\boldsymbol{\epsilon}}$ are the major and minor axes of the polarization ellipse, and $\hat{\boldsymbol{k}} \| \hat{\mathbf{z}}$ is the pulse propagation direction. The degrees of linear and circular polarization of the jth pulse are, respectively, $\ell_j \equiv (\mathbf{e}_j \cdot \mathbf{e}_j) = (1-\eta_j^2)/(1+\eta_j^2)$ and $\xi_j \equiv \mathrm{Im}[\mathbf{e}_j^* \times \mathbf{e}_j]_z = 2\eta_j/(1+\eta_j^2)$, where $\ell_j^2 + \xi_j^2 = 1$. We solve the two-electron time-dependent Schrödinger equation (TDSE) for an electric field $\boldsymbol{F}(t)$ of intensity 10^{14} W/cm^2 and carrier frequency $\omega = 1.323$ a.u., which is greater than the He binding energy, $E_b = 0.9037$ a.u. Each pulse has a temporal envelope $F_0(t) = F_0\cos^2(\pi t/T)$ with $-T/2 \le t \le T/2$, where $T \equiv n_p(2\pi/\omega) = 344$ as is the total pulse duration for $n_p = 3$ optical cycles. This corresponds to a spectral width [6] $\Delta\omega \simeq 1.44\omega/n_p \approx 17$ eV, and a FWHM in the intensity of $0.36T$, or 1.1 cycles. Such single-cycle attosecond pulses (having linear polarization) have been achieved experimentally [7–9], albeit with much lower intensity. However, the vortices we predict involve single-photon ionization processes; thus, the vortex patterns will occur for lower intensity pulses, although the photoelectron count rate will scale linearly with intensity.

We obtain the wave packet $\Psi(t)$ by solving the six-dimensional two-electron TDSE for the He atom interacting with two circularly polarized attosecond pulses using methods developed previously [6] for a single arbitrarily polarized attosecond pulse. Our method uses the finite-element discrete-variable representation combined with the real-space-product algorithm [10] as well as Wigner rotation transformations at each time step from the laboratory frame to the frame of the instantaneous electric field [11,12]. We extract the triply differential probability (TDP) [13] for single ionization of He to $\mathrm{He}^+(1s)$ from the wave packet $\Psi(T+\tau)$ (i.e., after the end of the two pulses) by projecting $\Psi(T+\tau)$ onto correlated field-free Jacobi matrix wave functions [14]. The TDP, $d^3W/d^3\mathbf{p} \equiv \mathcal{W}_{\xi_2}^{\xi_1}(\mathbf{p})$, for single electron ionization to the continuum with momentum $\mathbf{p} \equiv (p, \theta, \varphi)$ is

$$\frac{d^3W}{d^3\mathbf{p}} \equiv |\langle \Theta_{1s}^{(-)}(\mathbf{r}_1,\mathbf{r}_2,\mathbf{p})|\Psi(\mathbf{r}_1,\mathbf{r}_2,\mathbf{e}_{\phi_1},\mathbf{e}_{\phi_2},T+\tau)\rangle|^2, \quad (2)$$

where $\mathbf{e}_{\phi_j} \equiv \mathbf{e}_j e^{-i\phi_j}$, with $j = 1, 2$. We include four total angular momenta ($L = 0-3$), their azimuthal quantum numbers $|M| \le L$, and all combinations of individual electron orbital angular momenta $l_1, l_2 = 0$–5. Regardless of time delay τ, our numerical results show that only $M = +L$ (respectively, $M = -L$) states are populated for two identical pulses with $\xi_1 = \xi_2 = +1$ (respectively, $\xi_1 = \xi_2 = -1$). For two oppositely circularly polarized pulses (with $\xi_1 = -\xi_2 = \pm 1$) only $M = \pm L$ states are populated. In all cases, $^1P^o$ states give the dominant contribution (by 2 orders of magnitude) thus indicating our results stem from single photon ionization processes.

For our pulse parameters, first-order perturbation theory (PT) applies. The PT analysis of the problem, given in the Supplemental Material [15], is similar to that for ionization by a single pulse [19]. Below we present results of our PT analysis for two cases: (i) the two pulses have the same polarization $\mathbf{e}_1 = \mathbf{e}_2$; (ii) the pulses are circularly polarized in opposite directions, $\mathbf{e}_1 = \mathbf{e}_2^*$.

For two identically polarized pulses, $\ell_1 = \ell_2 = \ell$ and $\xi_1 = \xi_2 = \xi$. The TDP $d^3W/d^3\mathbf{p}$ is thus (see Supplemental Material [15])

$$\mathcal{W}_{\xi}^{\xi}(p,\theta,\varphi) = \frac{3W_p}{2\pi}(1 + \ell\cos 2\varphi)\sin^2\theta\cos^2(\Phi/2), \quad (3)$$

where the relative phase, Φ, is given by

$$\Phi = (E + E_b)\tau + (\phi_1 - \phi_2) \equiv (p^2/2 + E_b)\tau + \phi_{12}. \quad (4)$$

The dynamical parameter W_p in Eq. (3) depends only on the electron energy, $E = p^2/2$; it is independent of the momentum direction, $\hat{\mathbf{p}}$, and the pulse parameters $\mathbf{e}_1$, $\mathbf{e}_2$, τ, and $\phi_{12} = \phi_1 - \phi_2$. Consequently, the φ dependence of the TDP Eq. (3) is determined by the degree of linear polarization ℓ. For circularly polarized pulses $\eta = \pm 1$, $\xi = \pm 1$, and $\ell = 0$. Hence the TDP Eq. (3) is independent of φ and its polar angle plots in the polarization plane ($\theta = \pi/2$) have circularly symmetric patterns, as shown in Fig. 1 for two right-circularly polarized pulses with different CEPs for two time delays: $\tau = 0$ and $\tau = 500$ as. Owing to the dependence of the relative phase Φ on the time delay τ [cf. Eq. (4)], for $\tau = 0$ there is no structure in the momentum distribution. For $\tau = 500$ as, however, the Ramsey interference of the two electronic wave packets has a form similar to Newton's rings, i.e., maxima and minima along the radial direction in momentum space. (The interference pattern in Fig. 1(b) is similar to that found in interference of two identical optical beams [5].) Although the two pulses have different CEPs, owing to the circular symmetry, varying the relative CEP ϕ_{12} only changes the magnitude of the differential probability

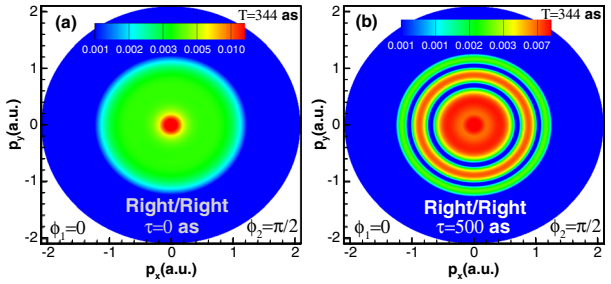

FIG. 1 (color online). Triply differential probability (TDP) $d^3W/d^3\mathbf{p}$ [see Eqs. (2), (3), and (4)] in the polarization plane for ionization of He by two right-circularly polarized pulses delayed in time by (a) $\tau = 0$; and (b) $\tau = 500$ as. Each pulse has carrier frequency $\omega = 36$ eV, $n_p = 3$ cycles with total duration $T = 344$ as, intensity $I = 10^{14}$ W/cm^2, and CEPs of $\phi_1 = 0$ and $\phi_2 = \pi/2$. The magnitudes in a.u. of the TDPs are indicated by the color scales in each panel.

$\mathcal{W}_{\xi}^{\xi}(p,\pi/2,\varphi)$ but has no effect on the pattern in the polarization plane. Averaging Eq. (3) over $\hat{\mathbf{p}}$, we obtain the single differential probability $dW/dE = pW_p[2\cos(\Phi/2)]^2$. Hence, the ionization probability for fixed ϕ_{12} can be controlled by varying the time delay τ [cf. Eq. (4)].

For oppositely circularly polarized pulses, $\mathbf{e}_1^* = \mathbf{e}_2$, $\ell_1 = \ell_2 = 0$, and $\xi_1 = -\xi_2 = \pm 1$. The TDP $d^3W/d^3\mathbf{p}$ takes the form (see Supplemental Material [15]):

$$\mathcal{W}_{\xi_2}^{\xi_1}(p,\theta,\varphi) = \frac{3W_p}{2\pi}\sin^2\theta\cos^2(\Phi/2 - \xi_1\varphi), \quad (5)$$

where $\xi_1 = -\xi_2 = \pm 1$ corresponds to a right-left (+) or a left-right (−) pair of oppositely circularly polarized pulses. In contrast to the case of identical pulses, the angle-averaged probability, $dW/dE = 2pW_p$, depends neither on the time delay, τ, nor the relative CEP, ϕ_{12}. The photoelectron angular distribution, Eq. (5), in the polarization plane ($\theta = 90°$) has the form of a *two-start* or *two-arm* spiral structure, as may be seen from the following considerations. From Eq. (5), the TDP $\mathcal{W}_{\xi_2}^{\xi_1}$ is maximal for $\Phi/2 - \xi_1\varphi = \Phi/2 + \xi_2\varphi = \pi n$ and is zero for $\Phi/2 - \xi_1\varphi = \Phi/2 + \xi_2\varphi = (2n+1)\pi/2$, where $n = 0, \pm 1, \pm 2, \ldots$, and $0 \le \varphi \le 2\pi$. Using Eq. (4), the p dependence of the polar angles φ at these maximum and zero values of $\mathcal{W}_{\xi_2}^{\xi_1}(p,\theta,\varphi)$ is

$$\varphi_n^{\max}(p) = \xi_2[\pi n - (\tau E_b + \phi_{12})/2 - \tau p^2/4],$$
$$\varphi_n^{\text{zero}}(p) = \xi_2[\pi/2 + \pi n - (\tau E_b + \phi_{12})/2 - \tau p^2/4]. \quad (6)$$

Equations (6) define Fermat (or Archimedean) spirals (or helixes) in the (p,φ) plane. As $\varphi_n^{\max}(p)$ and $\varphi_n^{\text{zero}}(p)$, shifted by the angle $\pi/2$ with respect to each other, vary with energy $p^2/2$ (through possibly many 2π cycles, depending upon τ), they trace out the maxima and the zeros of the TDP. Since $|\xi_2| = 1$, the pattern is a *two-arm* helical spiral, corresponding to $n = 0, 1$, as other values of

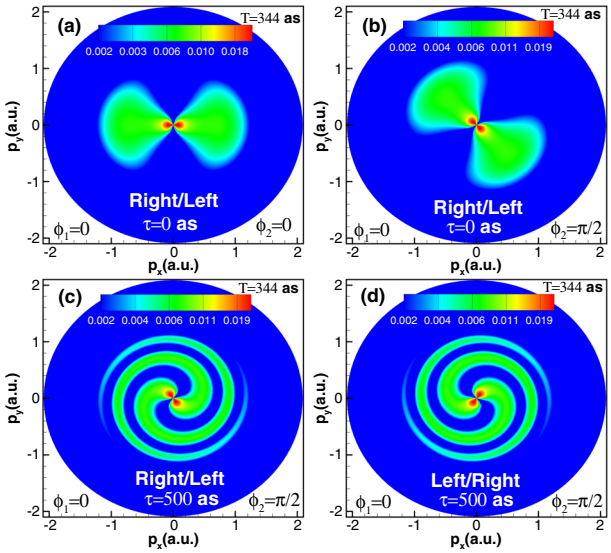

FIG. 2 (color online). Triply differential probability (TDP) $d^3W/d^3\mathbf{p}$ [see Eqs. (2), (4), and (5)] in the polarization plane for He ionization by (a),(b),(c) right-left and (d) left-right circularly polarized attosecond pulses. Top row results: time delay $\tau = 0$; bottom row results: $\tau = 500$ as. In (a), $\phi_1 = \phi_2 = 0$; in (b), (c), (d), $\phi_1 = 0$, $\phi_2 = \pi/2$. In all panels $\omega = 36$ eV, $n_p = 3$ cycles, $I = 10^{14}$ W/cm^2, and the magnitudes in a.u. of the TDPs are indicated by the color scales.

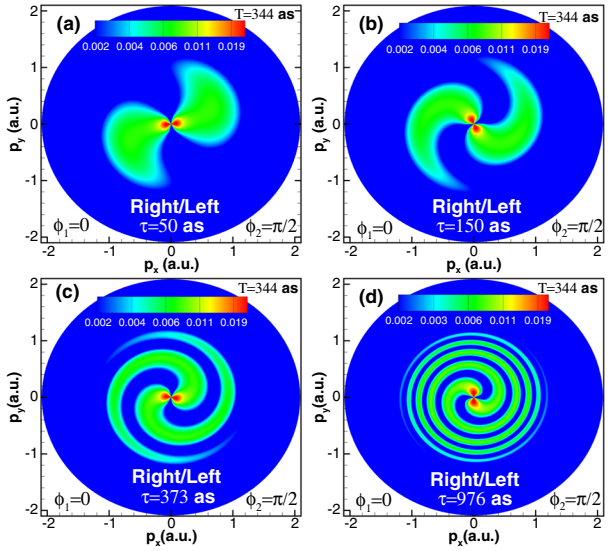

FIG. 3 (color online). Photoelectron momentum distributions $d^3W/d^3\mathbf{p}$ [see Eqs. (2), (4), and (5)] in the polarization plane for ionization of He by right-left circularly polarized attosecond pulses delayed in time by (a) $\tau = 50$ as; (b) $\tau = 150$ as; (c) $\tau = 373$ as; and (d) $\tau = 976$ as. Pulse parameters are the same as in Figs. 2(b) and 2(c). The magnitudes in a.u. of the TDPs are indicated by the color scales.

n replicate the same lines. Pulses with $\xi_1 = -\xi_2 = \pm 1$ correspond to right- (+) or left- (−) handed spirals. The Fermat spirals become wound more densely as τ increases.

Our numerical results for these PT predictions for two oppositely circularly polarized few-cycle attosecond pulses are shown in Figs. 2 and 3, where we plot the photoelectron momentum distributions in the polarization plane for various CEPs and time delays. Figures 2(a) and 2(b) are for zero time delay between the pulses and two relative CEPs ϕ_{12}. For $\tau = 0$, superposing two oppositely circularly polarized pulses gives a linearly polarized pulse and we observe in Fig. 2(a) the expected symmetric dipole pattern $[\propto \cos^2(\xi_1\varphi)]$ of the ionized electron momenta along the linear polarization axis, which for $\phi_{12} = 0$ is the p_x axis ($\varphi = 0, \pi$). A similar result is shown in Fig. 2(b) except that here $\phi_{12} = -\pi/2$ so that the linear polarization axis is rotated clockwise by $\varphi = \pi/4$, giving an angular distribution $\propto \cos^2(\phi_{12}/2 - \xi_1\varphi)$. For $\phi_{12} \neq 0$, a change in sign of ξ_1 will change the angular distribution, unlike when $\phi_{12} = 0$. This sensitivity to the helicity of ξ_1 is essential for producing vortices when the time delay is nonzero.

For a time delay of $\tau = 500$ as and $\phi_{12} = -\pi/2$, we obtain the vortices shown in Figs. 2(c) and 2(d) for right-left and left-right circularly polarized pulses, respectively. As discussed above, these are two-start Fermat spiral patterns with opposite handedness, i.e., counterclockwise in Fig. 2(c) and clockwise in Fig. 2(d). (For a 3D plot of the vortex pattern in Fig. 2(c), see Fig. 1 of the Supplemental Material [15].) As predicted by PT Eq. (6), the number and locations of the maxima and minima of the differential probability $\mathcal{W}^{\xi_1}_{\xi_2}(p, \pi/2, \varphi)$ in the polarization plane depend on the time delay τ, as shown in Fig. 3 for four additional values of τ. The results in Fig. 3 show that time delays of several hundred attoseconds are necessary to observe well-defined vortex patterns. As shown in the Supplemental Material [15], the broad bandwidth of attosecond pulses is necessary to observe the spiral patterns clearly.

Vortices in the probability distribution for a physical process are quite general phenomena [20,21]. The connection between a zero of the probability distribution and a zero of the system wave function is given by the so-called "imaging theorem" [21]. Velocity field vortices have been intensively studied for collision processes involving ionization of atoms and molecules by electron impact [21–23], proton impact [24], positron impact [25], ion impact [26], and both antiproton and photon impact [27]. Also, vortices associated with population transfers to excited and continuum states have been studied in the electron probability density of an atom subject to short linearly-polarized electric fields [27,28]. However, as noted by I. Bialynicki-Birula *et al.* [20], "We have to admit that vortex lines associated with wave functions are rather elusive objects." In particular, vortex lines in impact ionization amplitudes are not explicitly seen as vortices in the angular distributions. In contrast, for ionization by two oppositely circularly polarized pulses, the TDP vanishes along the two Fermat spiral arms in the (p_x, p_y) plane [cf. Eq. (6) for $\varphi_n^{\text{zero}}(p)$ for $n = 0, 1$]. These curves are thus a pair of vortex lines in the velocity field of the photoelectron wave function [21].

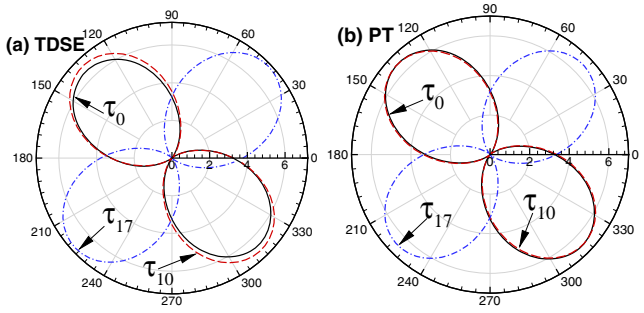

FIG. 4 (color online). Angular distributions $d^3W/d^3\mathbf{p}$ (in units of 10^{-3} a.u.) for a fixed photoelectron energy $E_1 = \omega - E_b$, produced by a pair of right-left circularly polarized attosecond pulses. Results in panel (a) are obtained by *ab initio* TDSE calculations [see Eq. (2)]; results in panel (b) are obtained using the PT formula (5) in which the dynamical parameter W_p is determined from our TDSE results for a *single* right-circularly polarized attosecond pulse including only the ${}^1P^o$ final state amplitude. In each panel, results are shown for three time delays: τ_0, τ_{10}, and τ_{17}, where $\tau_n = n\pi/\omega$.

The photoelectron vortex patterns in our TDPs in Figs. 2 and 3 are similar to the interference fringes of optical beams carrying orbital angular momentum of unity [5]. In both cases the interference patterns are two-start Fermat spirals whose orientation is determined by a relative phase difference. In our case, this phase difference Φ is determined by the energy $(p^2/2 + E_b)$, time delay τ, and ϕ_{12}, while in the optical case the relative phase is determined by the wave front curvature difference [5] (see Supplemental Material [15]). In neither case is the appearance of helical fringes caused by the polarization of either the optical or electronic waves. Indeed, in the optical case both light beams were linearly polarized [5], and in our electronic case, the electron states with $L_z = \pm 1$ are essentially equally populated upon ionization by the pair of oppositely circularly polarized attosecond pulses.

Figure 4 shows the time-delay periodicity of the photoelectron angular distributions in the polarization plane. Results of our numerical solutions of the TDSE in Fig. 4(a) are compared with the PT results in Fig. 4(b) for a *fixed* electron kinetic energy, $E_1 = \omega - E_b$. For a fixed relative CEP ϕ_{12} between the two pulses, the angular distribution is unchanged for time delays of $\tau_n = n\pi/(E + E_b)$ with n an even integer, as expected from the PT Eqs. (4) and (5). Figure 4(b) shows this PT result to be valid: the angular distributions for τ_0 and τ_{10} are identical. Our numerical results in Fig. 4(a) for these two time delays are nearly the same. This indicates the PT assumption that the second pulse sees the same initial state as the first pulse (i.e., the He ground state), instead of the state resulting from interaction of the He ground state with the first attosecond pulse, is valid to a very good approximation (especially given the greater sensitivity of differential probability results to theoretical approximations as compared to results for total probabilities). For time delays τ_n with odd integer n, the PT Eqs. (5) and (4) predict the angular distributions to be shifted by $\pi/2$ with respect to those for even integers n, as shown in Figs. 4(a) and 4(b). This sensitivity of the angular distributions to the time delay implies the ability to control the direction of ionization of electrons by adjusting the time delay between the two attosecond pulses.

Experimental observation of these vortex patterns in the photoelectron momentum distributions requires a pair of oppositely circularly polarized attosecond pulses with even low intensity but with control of the relative CEP and the time delay between the two pulses. The spectral width $\Delta\omega$ of each pulse should span the energies of several spiral fringes, i.e., $2\pi/\tau < \Delta\omega$ [see Eqs. (4), (5), and (6)]. Generation of circularly polarized harmonics in the extreme ultraviolet energy regime has recently been achieved [29]. Velocity map imaging or reaction microscope techniques can be used to measure the photoelectron momentum distribution. The sensitivity of these vortex patterns to the parameters of the pair of attosecond pulses makes them an ideal means of characterizing these pulses and of timing ultrafast processes. Finally, the He atom and other light atoms such as H, Li, and Be are ideal targets owing to the fact that they have only occupied subshells of $l = 0$ electrons, thus obviating (in the case of heavier atoms) effects of ionization of two or more subshells having different angular momenta by broad bandwidth attosecond pulses.

A. F. S. and J. M. N. D. gratefully acknowledge useful discussions with Cornelis Uiterwaal on optical vortices. Research of A. F. S. and J. M. N. D. is primarily supported by the U.S. Department of Energy (DOE), Office of Science, Basic Energy Sciences (BES), under Award No. DE-FG03-96ER14646; research of S. X. H. is supported by the DOE National Nuclear Security Administration under Award No. DE-NA0001944, the University of Rochester, and the New York State Energy Research and Development Authority; research of L. B. M. is supported by ERC-StG (Project No. 277767—TDMET) and the VKR Center of Excellence, QUSCOPE; research of N. L. M. and A. V. M. is supported by Russian Foundation for Basic Research Grant No. 13-02-00420 and by Ministry of Education and Science of the Russian Federation Project 1019. Computations were carried out using the Sandhills, Tusker, and Crane computing facilities of the Holland Computing Center at the University of Nebraska-Lincoln, as well as the Stampede supercomputer at the Texas Advanced Computing Center under NSF Grant No. TG-PHY-120003.

[1] N. F. Ramsey, A molecular beam resonance method with separated oscillating fields, Phys. Rev. **78**, 695 (1950).
[2] L. D. Noordam, D. I. Duncan, and T. F. Gallagher, Ramsey fringes in atomic Rydberg wave packets, Phys. Rev. A **45**, 4734 (1992).

[3] M. Strehle, U. Weichmann, and G. Gerber, Femtosecond time-resolved Rydberg wave-packet dynamics in the two-electron system calcium, Phys. Rev. A **58**, 450 (1998).
[4] M. Wollenhaupt, A. Assion, D. Liese, Ch. Sarpe-Tudoran, T. Baumert, S. Zamith, M. A. Bouchene, B. Girard, A. Flettner, U. Weichmann, and G. Gerber, Interferences of Ultrashort Free Electron Wave Packets, Phys. Rev. Lett. **89**, 173001 (2002).
[5] M. Harris, C. A. Hill, and J. M. Vaughan, Optical helices and spiral interference fringes, Opt. Commun. **106**, 161 (1994).
[6] J. M. Ngoko Djiokap, N. L. Manakov, A. V. Meremianin, S. X. Hu, L. B. Madsen, and A. F. Starace, Nonlinear Dichroism in Back-to-Back Double Ionization of He by an Intense Elliptically Polarized Few-Cycle Extreme Ultraviolet Pulse, Phys. Rev. Lett. **113**, 223002 (2014).
[7] G. Sansone, E. Benedetti, F. Calegari, C. Vozzi, L. Avaldi, R. Flammini, L. Poletto, P. Villoresi, C. Altucci, R. Velotta, S. Stagira, S. De Silvestri, and M. Nisoli, Isolated single-cycle attosecond pulses, Science **314**, 443 (2006).
[8] E. Goulielmakis, M. Schultze, M. Hofstetter, V. S. Yakovlev, J. Gagnon, M. Uiberacker, A. L. Aquila, E. M. Gullikson, D. T. Atwood, R. Kienberger, F. Krausz, and U. Kleineberg, Single-cycle nonlinear optics, Science **320**, 1614 (2008).
[9] K. Zhao, Q. Zhang, M. Chini, Y. Wu, X. Wang, and Z. Chang, Tailoring a 67 attosecond pulse through advantageous phase-mismatch, Opt. Lett. **37**, 3891 (2012).
[10] S. X. Hu, Optimizing the FEDVR-TDCC code for exploring the quantum dynamics of two-electron systems in intense laser pulses, Phys. Rev. E **81**, 056705 (2010).
[11] H. G. Muller, An efficient propagation scheme for the time-dependent Schrödinger equation in the velocity gauge, Laser Phys. **9**, 138 (1999).
[12] T. K. Kjeldsen, L. A. A. Nikolopoulos, and L. B. Madsen, Spectral and partial-wave decomposition of time-dependent wave functions on a grid: Photoelectron spectra of H and H_2^+ in electromagnetic fields, Phys. Rev. A **75**, 063427 (2007).
[13] L. B. Madsen, L. A. A. Nikolopoulos, T. K. Kjeldsen, and J. Fernández, Extracting continuum information from $\Psi(t)$ in time-dependent wave-packet calculations, Phys. Rev. A **76**, 063407 (2007).
[14] J. M. Ngoko Djiokap, S. X. Hu, W.-C. Jiang, L.-Y. Peng, and A. F. Starace, Enhanced asymmetry in few-cycle attosecond pulse ionization of He in the vicinity of autoionizing resonances, New J. Phys. **14**, 095010 (2012).
[15] See Supplemental Material at http://link.aps.org/supplemental/10.1103/PhysRevLett.115.113004 for a more detailed derivation of our PT equations and for an illustration of the time-delay sensitivity of the photoelectron energy distributions; the Supplemental Material includes Refs. [16–18].
[16] V. B. Berestetskii, E. M. Lifshitz, and L. P. Pitaevskii, *Quantum Electrodynamics*, 2nd ed. (Pergamon Press, Oxford, 1982).
[17] A. S. Davydov, *Quantum Mechanics*, 2nd ed. (Pergamon Press, Oxford, 1976).
[18] A. F. Starace, Theory of Atomic Photoionization, in *Handbuch der Physik*, edited by W. Mehlhorn, Vol. 31 (Springer-Verlag, Berlin, 1982), pp. 1–121.
[19] E. A. Pronin, A. F. Starace, M. V. Frolov, and N. L. Manakov, Perturbation theory analysis of attosecond photoionization, Phys. Rev. A **80**, 063403 (2009).
[20] I. Bialynicki-Birula, Z. Bialynicka-Birula, and C. Sliwa, Motion of vortex lines in quantum mechanics, Phys. Rev. A **61**, 032110 (2000).
[21] S. J. Ward and J. H. Macek, Effect of a vortex in the triply differential cross section for electron-impact K-shell ionization of carbon, Phys. Rev. A **90**, 062709 (2014).
[22] J. H. Macek, J. B. Sternberg, S. Y. Ovchinnikov, and J. S. Briggs, Theory of Deep Minima in $(e, 2e)$ Measurements of Triply Differential Cross Sections, Phys. Rev. Lett. **104**, 033201 (2010).
[23] J. M. Feagin, Vortex kinematics of a continuum electron pair, J. Phys. B **44**, 011001 (2011).
[24] J. H. Macek, J. B. Sternberg, S. Y. Ovchinnikov, T.-G. Lee, and D. R. Schultz, Origin, Evolution, and Imaging of Vortices in Atomic Processes, Phys. Rev. Lett. **102**, 143201 (2009).
[25] F. Navarrete, R. Della Picca, J. Fiol, and R. O. Barrachina, Vortices in ionization collisions by positron impact, J. Phys. B **46**, 115203 (2013).
[26] L. Ph. H. Schmidt, C. Goihl, D. Metz, H. Schmidt-Böcking, R. Dörner, S. Yu. Ovchinnikov, J. H. Macek, and D. R. Schultz, Vortices Associated with the Wave Function of a Single Electron Emitted in Slow Ion-Atom Collisions, Phys. Rev. Lett. **112**, 083201 (2014).
[27] S. Y. Ovchinnikov, J. H. Macek, and D. R. Schultz, Hydrodynamical interpretation of angular momentum and energy transfer in atomic processes, Phys. Rev. A **90**, 062713 (2014).
[28] S. Y. Ovchinnikov, J. B. Sternberg, J. H. Macek, T.-G. Lee, and D. R. Schultz, Creating and Manipulating Vortices in Atomic Wave Functions with Short Electric Field Pulses, Phys. Rev. Lett. **105**, 203005 (2010).
[29] O. Kfir, P. Grychtol, E. Turgut, R. Knut, D. Zusin, D. Popmintchev, T. Popmintchev, H. Nembach, J. M. Shaw, A. Fleischer, H. Kapteyn, M. Murnane, and O. Cohen, Generation of bright phase-matched circularly polarized extreme ultraviolet high harmonics, Nat. Photonics **9**, 99 (2014).